Chemical Science

EDGE ARTICLE

View Article Online
View Journal | View Issue

Cite this: *Chem. Sci.*, 2019, **10**, 5114

All publication charges for this article have been paid for by the Royal Society of Chemistry

Guest recognition enhanced by lateral interactions†

Tianyu Jiao,[ab] Kang Cai,[b] Zhichang Liu,[c] Guangcheng Wu,[a] Libo Shen,[a] Chuyang Cheng,[b] Yuanning Feng,[b] Charlotte L. Stern,[b] J. Fraser Stoddart*[bde] and Hao Li*[a]

Received 1st February 2019
Accepted 11th April 2019

DOI: 10.1039/c9sc00591a

rsc.li/chemical-science

A hexacationic triangular covalent organic cage, **AzaEx²Cage**$^{6+}$, has been synthesized by means of a tetrabutylammonium iodide-catalyzed S_N2 reaction. The prismatic cage is composed of two triangular 2,4,6-triphenyl-1,3,5-triazine (**TPT**) platforms bridged face-to-face by three 4,4′-bipyridinium (**BIPY**$^{2+}$) spacers. The rigidity of these building blocks leads to a shape-persistent cage cavity with an inter-platform distance of approximately 11.0 Å. This distance allows the cage to accommodate two aromatic guests, each of which is able to undergo π–π interactions with one of the two **TPT** platform simultaneously, in an A–D–D–A manner. In the previously reported prism-shaped cage, the spacers (pillars) are often considered passive or non-interactive. In the current system, the three **BIPY**$^{2+}$ spacers are observed to play an important role in guest recognition. Firstly, the **BIPY**$^{2+}$ spacers are able to interact with the carbonyl group in a pyrene-1-carbaldehyde (**PCA**) guest, by introducing lateral dipole–cation or dipole–dipole interactions. As a consequence, the binding affinity of the cage towards the **PCA** guest is significantly larger than that of pyrene as the guest, even although the latter is often considered to be a better π-electron donor. Secondly, in the case of the guest 1,5-bis[2-(2-(2-(2-hydroxyethoxy)ethoxy)ethoxy)ethoxy]naphthalene (**BH4EN**), the pillars can provide higher binding forces compared to the **TPT** platform. Hence, peripheral complexation occurs when **AzaEx²Cage**$^{6+}$ accommodates **BH4EN** in MeCN. Thirdly, when both **PCA** and **BH4EN** are added into a solution of **AzaEx²Cage**$^{6+}$, inclusion and peripheral complexation occur simultaneously to **PCA** and **BH4EN** respectively, even though the accommodation of the former guest seems to attenuate the external binding of the latter. This discovery of the importance of lateral interactions highlights the relationship between the electrostatic properties of a highly charged host and its complexation behavior, and as such, provides insight into the design of more complex hosts that bind guests in multiple locations and modes.

Introduction

Cyclophanes, such as calix[*n*]arenes,[1] oxacalixarenes,[2] resorcinarenes,[3] pillar[*n*]arene,[4] calixpyrroles,[5] as well as cationic ones,[6] including cyclobis(paraquat-*p*-phenylene) (**CBPQT**$^{4+}$)[7] and its extended counterparts,[8] represent one of the major focuses in the field of supramolecular chemistry. In the frameworks of these cyclophanes, various arenes are connected by a number of aliphatic linkers such as methylene units, resulting in relatively rigid and preorganized cavities where guest encapsulation could occur without significant entropy loss. For example, in the case of **CBPQT**$^{4+}$, π-electron-deficient 4,4′-bipyridinium (**BIPY**$^{2+}$) are separated by two *p*-xylene spacers in a face-to-face manner by approximately 7 Å, which is two times longer than a typical π–π interaction distance. These geometrical properties imply that **CBPQT**$^{4+}$ could accommodate a π-conjugated guest within its cavity, where π–π interactions[9] could occur between the guest and both the two **BIPY**$^{2+}$ platforms in the host.

These kind of host–guest recognition features of **CBPQT**$^{4+}$ and its homologous cyclophanes can be used to fulfill various tasks, including the construction of molecular switches[10] and machines[11] in the form of rotaxanes[12] and catenanes,[13] water purification *via* the extraction of aromatic compounds into the host,[14] and the stabilization of unusual guest conformations.[15] There are still several limitations, however, in the design principles of these cyclophanes.

[a]*Department of Chemistry, Zhejiang University, Hangzhou 310027, P. R. China. E-mail: lihao2015@zju.edu.cn*

[b]*Department of Chemistry, Northwestern University, 2145 Sheridan Road, Evanston, Illinois 60208, USA. E-mail: stoddart@northwestern.edu*

[c]*School of Science, Westlake University, 18 Shilongshan Road, Hangzhou 310024, P. R. China*

[d]*Institute for Molecular Design and Synthesis, Tianjin University, Tianjin 300072, P. R. China*

[e]*School of Chemistry, University of New South Wales, Sydney, NSW 2052, Australia*

† Electronic supplementary information (ESI) available. CCDC 1858887–1858890 and 1858892. For ESI and crystallographic data in CIF or other electronic format see DOI: 10.1039/c9sc00591a

Firstly, the spacers that connect the π-electron-deficient moieties often behave as "passive" or non-interactive building blocks in terms of molecular recognition – except for a few examples where these spacers can take part in relatively weak [C–H···π] interactions.[16] Secondly, in most cases, host–guest complexation occurs within the host cavity wherein the interactions between the guests and the two platforms occur simultaneously. Furthermore, these interactions are often strengthened by solvophobic effects in polar solvents. As a consequence, most of these cages or rings only have one binding mode or site. There are very few examples[17] of guests binding externally to these hosts.

In the current work, we report the design and synthesis of a hexacationic triangular prism, **AzaEx^{2}Cage**$^{6+}$, which is composed of two **TPT** platforms connected face-to-face by three **BIPY**$^{2+}$ pillars. The distance between the two platforms is approximately 11.0 Å, which is approximately three-times larger than a typical π–π interaction distance, implying that the cavity in this prism could encapsulate two aromatic guest molecules such as pyrene. Interestingly, in contrast to previously reported hosts that contain phenyl or biphenyl spacers, the **BIPY**$^{2+}$ spacers in **AzaEx^{2}Cage**$^{6+}$ play a more important role in host–guest complexation.

The host exhibits significantly better binding affinity towards pyrene-1-carbaldehyde (**PCA**) than towards pyrene in both organic solvents and water because the former guest contains a partially negatively charged carbonyl group that can undergo dipole–cation or dipole–dipole interactions with the positively charged **BIPY**$^{2+}$ pillars. Furthermore, the **BIPY**$^{2+}$ pillars allow the cage to form an external complex with 1,5-bis[2-(2-(2-(2-hydroxyethoxy)ethoxy)ethoxy)ethoxy]naphthalene (**BH4EN**), a guest containing two tetraethylene glycol chains grafted onto a 1,5-dioxynaphthalene (**DNP**) moiety. This external binding is driven by the donor–acceptor interactions between the **DNP** unit in the guest and the **BIPY**$^{2+}$ pillar in the host, as well as hydrogen bonding between the glycol oxygen atoms and the relatively acidic protons in the **BIPY**$^{2+}$ units. The assumption that the **DNP** unit prefers to interact with the more electron-deficient **BIPY**$^{2+}$ pillar instead of the triazine-containing platform inside the cage is supported by both single-crystal X-ray diffraction analysis and theoretical calculations. Furthermore, guest encapsulation and external binding to the cage occur simultaneously in the presence of both **PCA** and **BH4EN**, even though binding of the latter slightly decreases upon encapsulation of the former.

We envision that our findings will promote the fundamental understanding, and thus design, of hosts that are able to accommodate guests in multiple modes or sites.

Experimental section

Synthesis and characterization of AzaEx^{2}Cage·6PF$_6$

2,4,6-Tris[4-(bromomethyl)phenyl]-1,3,5-triazine (**TBT**) – a molecule that comprises three benzyl bromide functions grafted onto a **TPT** moiety – was synthesized in high yield from the acid-catalyzed trimerization of 4-cyanobenzyl bromide.[18] **TBT** was added slowly into a refluxing solution containing a 40-fold excess of 4,4′-bipyridine in MeCN and DMF (1 : 1 v/v) at 90 °C in several aliquots over the course of 6 h, yielding the triscationic compound **TBTP**·3PF$_6$ after counterion exchange. A 1 : 1 mixture of **TBT** and **TBTP**·3PF$_6$ was then combined and heated at 80 °C in MeCN in the presence of 0.2 equiv. of tetrabutylammonium iodide (TBAI) as a catalyst, leading to the formation (Scheme 1) of a substantial amount of yellow precipitate. The ^{1}H NMR spectrum of the precipitate, recorded in CD_3SOCD_3, indicates that the cage **AzaEx^{2}Cage**$^{6+}$, the counterions of which could be either Br^-, I^- or PF_6^-, represents the major product in the precipitate, along with a variety of oligomers or polymers as the minor products. Pure **AzaEx^{2}Cage**·6PF$_6$ was obtained in 16% yield by means of silica gel chromatography (1% NH_4PF_6 in MeCN (w/v)), before which counterion exchange was performed. Two more water-soluble counterparts, namely **AzaEx^{2}Cage**·6Cl and **AzaEx^{2}Cage**·6CF$_3$CO$_2$, were then obtained from **AzaEx^{2}Cage**·6PF$_6$ by counterion exchange.

Results and discussion

AzaEx^{2}Cage·6PF$_6$ was fully characterized by NMR spectroscopy, high-resolution mass spectrometry (HRMS), and X-ray diffraction analysis. Its ^{1}H NMR spectrum is remarkably simple (Fig. 1b), indicating that the cage has averaged D_{3h} symmetry in solution.

Single crystals of both **AzaEx^{2}Cage**·6PF$_6$ and **AzaEx^{2}Cage**·6CF$_3$CO$_2$ were obtained by vapor diffusion of ^{i}Pr$_2$O into the corresponding MeCN solutions. Crystal twinning was observed, however, in the case of the former crystals (Fig. S40 and S41†). As expected, in the solid-state structure (Fig. 2) of **AzaEx^{2}Cage**·6CF$_3$CO$_2$, the two **TPT** platforms in a cage framework are separated by a distance of approximately 11.0 Å, which is three-times larger than a typical π–π interaction distance,[19]

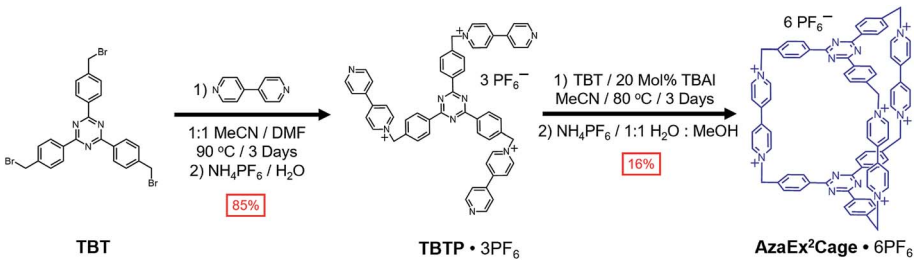

Scheme 1 Synthesis of AzaEx^{2}Cage·6PF$_6$ from TBT.

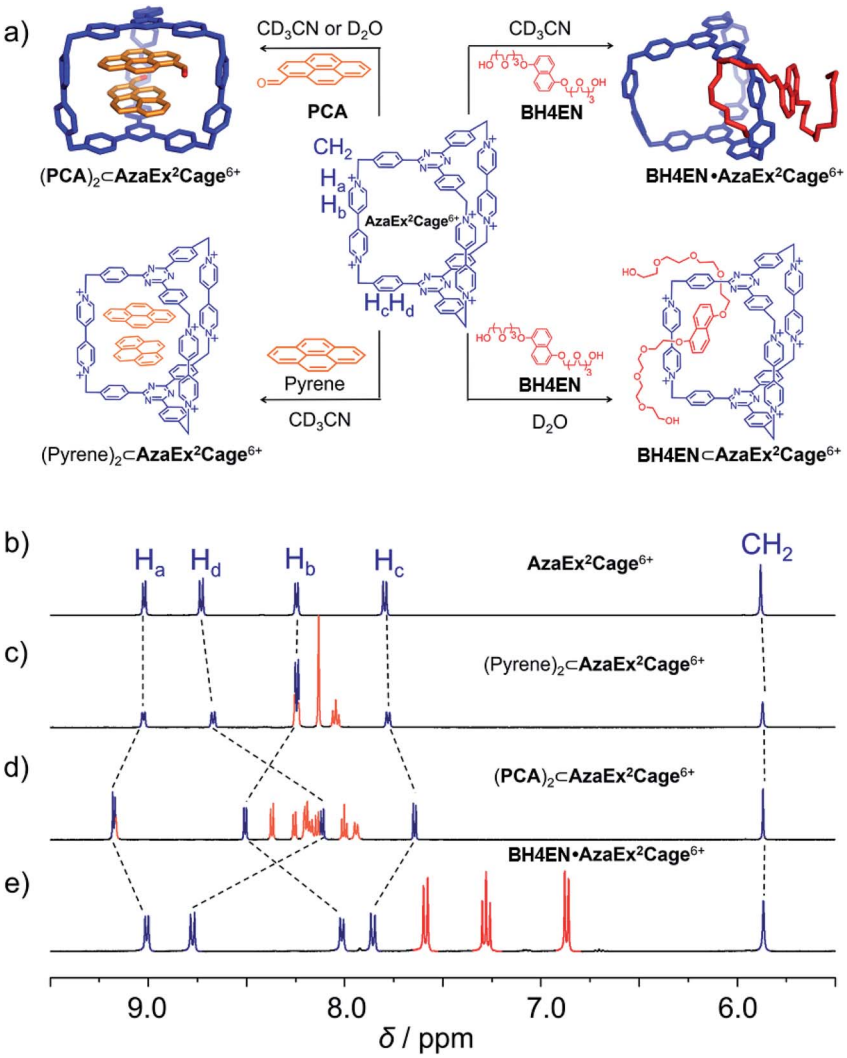

Fig. 1 (a) Schematic representation of the ability of **AzaEx^{2}Cage**$^{6+}$ to recognize a variety of guests, including pyrene, **PCA**, and **BH4EN**. In the cases of pyrene and **PCA**, 2 : 1 complexes are formed, even though the ability of the cage to host the former guest is much weaker. In the case of **BH4EN**, the complex **BH4EN**·**AzaEx^{2}Cage**$^{6+}$ forms in a peripheral and inclusion manner in CD_3CN and D_2O, respectively. ^{1}H NMR spectra of **AzaEx^{2}Cage**·$6PF_6$ (500 MHz, 1.0 mM in CD_3CN, 298 K) (b) before and after adding (c) pyrene (8.4 equiv.), (d) **PCA** (10.8 equiv.), and (e) **BH4EN** (11.4 equiv.). The resonances of the protons in **AzaEx^{2}Cage**$^{6+}$ are labeled in the corresponding spectra. Addition of pyrene and **PCA** results in upfield shifts of the resonances of the phenylene residues (H_c and H_d) in **AzaEx^{2}Cage**$^{6+}$, while the presence of **BH4EN** leads to upfield shifting of the resonances for the protons on **BIPY**$^{2+}$ (H_a and H_b).

indicating that the cage is able to accommodate two aromatic guests in an A–D–D–A (A = acceptor; D = donor) manner. The distance between two adjacent methylene linkers within each **TPT** platform is around 11.6 Å. As a result, the cage framework has three relatively large (11.0 Å × 11.6 Å) rectangular pore windows. These large windows allow potential guests to undergo relatively fast association/dissociation with the cage. The CF_3CO_2 counterions are located close to the **BIPY**$^{2+}$ pillars. Hydrogen-bonding interactions occur between the $CF_3CO_2^-$ counterions and the protons of the cage in the solid state. Furthermore, pairs of adjacent cage frameworks undergo stacking with each other, driven by π–π interactions between a triazine unit in the platform of one cage and a phenyl moiety of the other.

Cyclic voltammetry (CV) analysis (Fig. S36a†) of **AzaEx^{2}Cage**·$6PF_6$ in degassed DMF reveals two consecutive reversible redox processes. The reduction processes at −0.264 and −0.662 V can be assigned to two consecutive three-electron reductions, *i.e.*, **BIPY**$^{2+}$/**BIPY**$^{+\bullet}$ and **BIPY**$^{+\bullet}$/**BIPY**^{0}, by three identical **BIPY**$^{2+}$ pillars in a cage. The simultaneous reduction of the three pillars indicates the absence of electron communication between the **BIPY**$^{2+}$ units within the cage framework.

The UV-Vis-NIR absorption spectrum (Fig. S36b†) of **AzaEx^{2}Cage**$^{3(+\bullet)}$ was obtained by adding Zn dust as a reductant to a solution of **AzaEx^{2}Cage**·$6PF_6$ in MeCN. The spectrum is similar to that of 4,4′-dimethylviologen radical cations, further demonstrating that neither radical pairing nor dimerization occurs between any two of the three **BIPY**$^{+\bullet}$ pillars of the cage **AzaEx^{2}Cage**$^{3(+\bullet)}$. The absence of intramolecular radical pairing interactions[20] is not surprising because the three **BIPY**$^{+\bullet}$ units are separated by approximately 11.6 Å within the rigid cage framework.

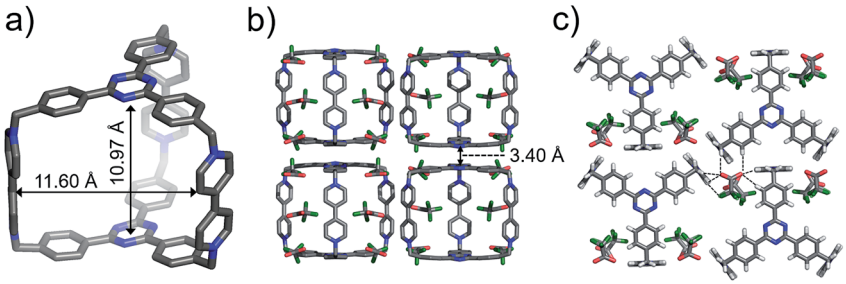

Fig. 2 Solid-state (super)structures of **AzaEx^{2}Cage**·6CF_3CO_2 obtained by single-crystal X-ray crystallography. (a) Stick representation of **AzaEx^{2}Cage^{6+}**, $CF_3CO_2^-$ counterions are omitted for the sake of clarity. (b and c) Side-on views of the packing structure revealing that π–π and hydrogen-bonding interactions play important roles in the crystal packing. The close contacts in the range of 2.22–2.46 Å between $CF_3CO_2^-$ counteranions and the protons in the cage indicate the occurrence of Hydrogen-bonding interactions, which are labeled with dashed lines. Hydrogen atoms and disordered solvent molecules are omitted for the sake of clarity. C, gray; N, blue; F, green; O, red.

Host–guest recognition

We first investigated the ability of **AzaEx^{2}Cage^{6+}** to accommodate two π-electron-rich guests, since the two **TPT** platforms are π-electron acceptors. The ^{1}H NMR resonances for **AzaEx^{2}Cage**·6PF_6 recorded in CD_3CN exhibit only relatively small shifts upon addition of different guests, including pyrene, triphenylene, and perylene. For example, upon addition of 8.37 equiv. of pyrene, the resonances of the H_c and H_d protons in the phenylene residues of **AzaEx^{2}Cage**·6PF_6 undergo (Fig. 1c) upfield shifts of just −0.02 and −0.06 ppm, respectively. These findings indicate that the ability of **AzaEx^{2}Cage^{6+}** to accommodate pyrene within its cavity is remarkably small. Side-on interactions between the host platforms and the guests in a external manner may also contribute to the upfield shifts of the cage proton resonances in the ^{1}H NMR spectra, at least partially. For example, after adding 30 equiv. of pyrene into a solution of **TBT** in CD_3CN, the resonances of the corresponding phenylene protons undergo upfield shifts of −0.02 and −0.04 ppm, respectively. In fact, the binding constants of **AzaEx^{2}Cage^{6+}** to two pyrene molecules in CD_3CN, *i.e.*, K_1 and K_2, are too low to be determined accurately by means of ^{1}H NMR titration experiments. A 1 : 1 binding model was employed to fit the NMR titration data, for which $K_{eq} = 11.1 \pm 0.2$ M^{-1} was determined (Fig. S22 and S23†). Several attempts were made to obtain single crystals of the complex (pyrene)$_2$⊂**AzaEx^{2}Cage^{6+}** by vapor diffusion of $^iPr_2O$ into MeCN solutions containing both pyrene and **AzaEx^{2}Cage**·6PF_6 at different guest-to-host ratios ranging from 5 : 1 to 40 : 1. All of these attempts, however, yielded only a few single crystals corresponding to "empty" **AzaEx^{2}Cage**·6PF_6 cages, further supporting our conclusion that the binding affinity of (pyrene)$_2$⊂**AzaEx^{2}Cage^{6+}** is at best very weak.

We also envisioned that **AzaEx^{2}Cage**·6Cl might be capable of accommodating pyrene in water by taking advantage of the hydrophobic effect. After sonicating suspensions of pyrene in D_2O solutions of **AzaEx^{2}Cage**·6Cl (1.0 mM) at both room temperature and 80 °C for no less than 5 h, however, no resonances corresponding to pyrene were observed in the ^{1}H NMR spectra. In addition, the resonances of the cage protons remained almost completely unshifted. These results are in contrast to our previously reported findings, *i.e.*, that the two smaller cages, namely **ExCage^{6+}** (ref. 14) and **AzaExCage^{6+}**,[21] can encapsulate a variety of polycyclic aromatic hydrocarbons with remarkably high binding constants in both organic solvents and water. For example, the K_a values for pyrene⊂**ExCage^{6+}** and pyrene⊂**AzaExCage^{6+}** are 6.77 × 10^5 (ref. 14) and 4.93 × 10^5 M^{-1},[21] respectively, in MeCN. The lower binding affinity in the case of **AzaEx^{2}Cage^{6+}** could be explained by the facts that (i) the **TPT** platform of **AzaEx^{2}Cage^{6+}** is a weaker π-electron acceptor than the more electron-deficient triscationic counterparts such as 1,3,5-pyridinium-phenyl in **ExCage^{6+}** and 2,4,6-pyridinium-1,3,5-triazine in **AzaExCage^{6+}**, (ii) the formation the 2 : 1 complex (pyrene)$_2$⊂**AzaEx^{2}Cage^{6+}** is less entropically favored than formation of the 1 : 1 complexes pyrene⊂**ExCage^{6+}** and pyrene⊂**AzaExCage^{6+}** (*i.e.*, **ExCage^{6+}** and **AzaExCage^{6+}** have more preorganized cavities for encapsulating pyrene guests) and (iii) the A–D–D–A binding mode in the case of (pyrene)$_2$⊂**AzaEx^{2}Cage^{6+}** involves a less favored D–D interaction, making its formation more energetically demanding than that of the A–D–A mode that occurs in both pyrene⊂**ExCage^{6+}** and pyrene⊂**AzaExCage^{6+}**.

Pyrene-1-carbaldehyde (**PCA**) is considered to be a weaker π-electron donor than pyrene, since it contains an electron-withdrawing formyl group. Surprisingly, **PCA** undergoes significantly stronger binding within the cavity of **AzaEx^{2}Cage**·6PF_6 compared to that of pyrene. For example, upon addition of 10.8 equiv. of **PCA** to a CD_3CN solution of **AzaEx^{2}Cage**·6PF_6 (Fig. 1d), the resonances of the H_c and H_d protons in the platforms of the cage undergo much more significant upfield shifts, *i.e.*, Δδ for H_c and H_d are −0.154 and −0.618 ppm, respectively, compared with −0.02 and −0.06 ppm, respectively, when 8.37 equiv. of pyrene is added (Fig. 1c). The upfield shifts reveal the presence of π–π interactions between the **TPT** platform and the pyrene moiety in the guest, providing the phenylene units in the platform with a magnetically shielded environment. Only one set of sharp resonances corresponding to either the host or the guest is observed in the ^{1}H NMR spectra (Fig. 1d and 3b), regardless of the host-to-guest ratio, indicating that host–guest association/dissociation occurs relatively rapidly on the ^{1}H NMR timescale. This observation is consistent with the solid-state

structure of **AzaEx²Cage**$^{6+}$ – *i.e.*, each cage contains three large pore windows allowing for rapid guest exchange.

^{1}H NMR titration experiments (Fig. 3b and c) revealed that the binding constants for the formation of (**PCA**)$_2\subset$**AzaEx²Cage**$^{6+}$ in CD_3CN, *i.e.*, K_1 and K_2, are 23 ± 3 and 730 ± 160 M^{-1}, respectively. The positive cooperativity effect is not surprising, given that the cage cavity with a length of 11 Å is too large and less preorganized to accommodate the first guest, which is able to undergo π–π interactions with only one of the two platforms in the host. After accommodation of the first guest, the cavity becomes smaller in size and therefore more complementary towards binding of the second guest molecule. In addition, the encapsulation of the second guest is driven by an extra guest–guest π–π interaction, which does not occur in the case of the first guest. The 2 : 1 complex (**PCA**)$_2\subset$**AzaEx²Cage**$^{6+}$ forms exclusively in D_2O upon sonicating **PCA** solid in a D_2O solution of **AzaEx²Cage**·6Cl (1.0 mM) at room temperature. Measuring the integration of the resonances for the protons corresponding to both the host and guest in the ^{1}H NMR spectrum (Fig. 3d) confirms the 1 : 2 host-to-guest stoichiometry of the complex, which is largely a result of the low solubility of the unbound guest in water. The 2D DOSY spectrum (Fig. 3d) further confirms the formation of the complex (**PCA**)$_2\subset$**AzaEx²Cage**$^{6+}$. In addition, in water, the resonance for the formyl proton in PCA undergoes a remarkable upfield shift, *i.e.*, $\delta = 8.41$ ppm; $\Delta\delta \approx 2$ ppm. This observation indicates that a short contact occurs between the aldehyde and one of the viologen pillars in the host. The latter unit thus provides a magnetically shielded chemical environment for the former group, which supports our assumption that the formyl group can undergo cation–dipole interactions with one of the viologen pillars.

Single crystals of (**PCA**)$_2\subset$**AzaEx²Cage**·6PF_6 suitable for X-ray diffraction were obtained by vapor diffusion of $^iPr_2O$ into its MeCN solution at 4 °C over 3 days, providing unambiguous evidence for the formation of a 2 : 1 complex (Fig. 4). As expected, two guest molecules are accommodated within the cavity of the cage framework. π–π Stacking interactions occur between the two platforms in the host and the two guests in an A–D–D–A manner, as inferred from the observation that the distances between triazine/pyrene, pyrene/pyrene, and pyrene/triazine are 3.42, 3.46, and 3.46 Å, respectively. The closest contacts between the two carbonyl oxygen atoms and the corresponding **BIPY**$^{2+}$ pillars of the host are 2.78 and 3.01 Å, indicating the occurrence of dipole–cation or dipole–dipole interactions. This secondary interaction is responsible for the enhanced binding affinities of **PCA** with the cage cavity relative

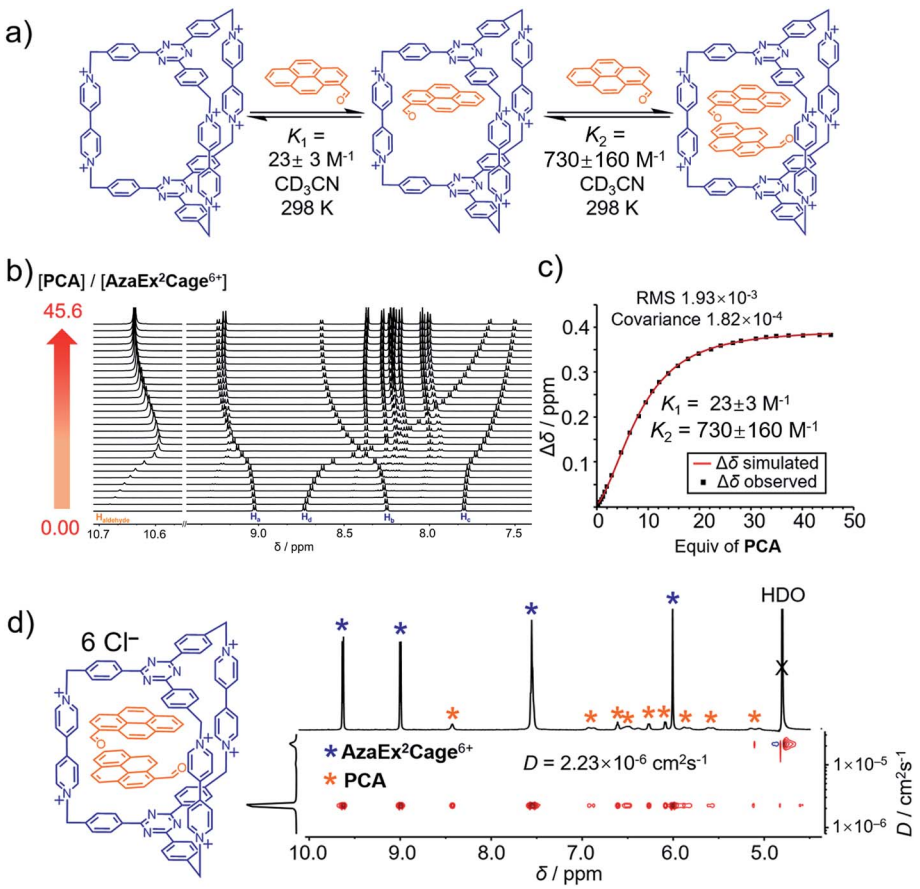

Fig. 3 (a) Schematic representation of the ability of **AzaEx²Cage**$^{6+}$ to accommodate two **PCA** guests, in which the corresponding binding constants K_1 and K_2 determined by ^{1}H NMR spectroscopy in CD_3CN at room temperature are shown. (b) Stacked ^{1}H NMR spectra of **AzaEx²Cage**·6PF_6 in CD_3CN upon addition of 0 to 45.6 equiv. of **PCA** relative to **AzaEx²Cage**$^{6+}$. (c) Plot of the downfield resonance shifts of H_b protons in **AzaEx²Cage**$^{6+}$ ($\Delta\delta$) *versus* the amount of **PCA** guest added relative to **AzaEx²Cage**$^{6+}$. [**AzaEx²Cage**·6PF_6] = 0.904 mM for all spectra. (d) 2D DOSY spectrum of the (**PCA**)$_2\subset$**AzaEx²Cage**$^{6+}$ recorded in D_2O.

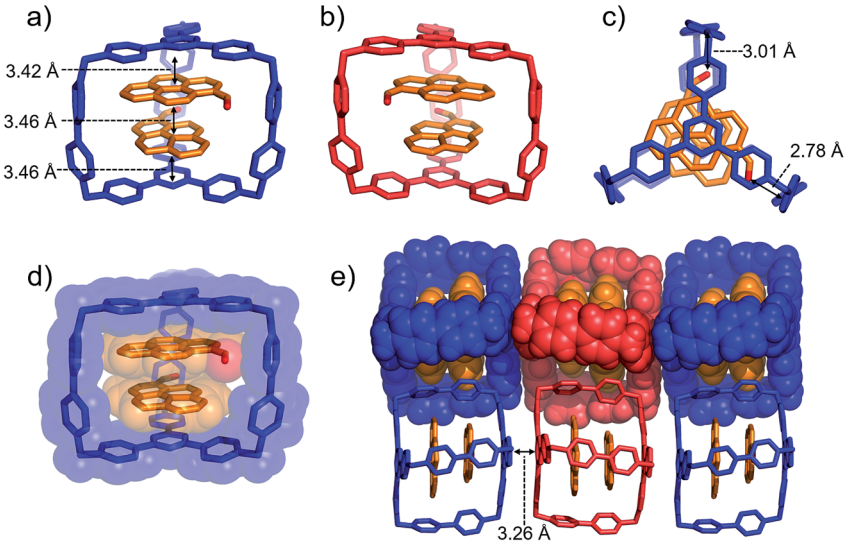

Fig. 4 (a) Side-on stick diagrams view of the crystal structures of $(PCA)_2 \subset AzaEx^2Cage^{6+}$ forms with different chirality including (a) *R* (blue) and (b) *S* (red). The axial chirality of the complex results from the different relative rotation directions of the carbonyl groups in the two **PCA** guests within the cage cavity. The interplane distances between the platforms in the host and the two guests are 3.42, 3.46, and 3.46 Å, indicating the occurrence of π–π stacking interactions. (c) Top view of the X-ray crystal structure of $(PCA)_2 \subset AzaEx^2Cage^{6+}$. The distances between the two carbonyl oxygen atoms and the corresponding $BIPY^{2+}$ pillars are 2.78 and 3.01 Å, respectively, indicating the occurrence of dipole–cation or dipole–dipole interactions. (d) Side-on stick diagram view overlaid with a space-filling representation of the crystal structure of $(PCA)_2 \subset^{\star} AzaEx^2Cage^{6+}$. (e) Side view of the crystal lattice of $(PCA)_2 \subset AzaEx^2Cage \cdot 6PF_6$ showing that complexes of different chirality undergo stacking with each other, making the crystal lattice a racemic mixture. PF_6^- counterions are omitted for the sake of clarity.

to those of pyrene. It is noteworthy that, in the solid state, the two carbonyl groups of the two guests interact with two different $BIPY^{2+}$ pillars in the cage in order to minimize the repulsion between the partially anionic carbonyl oxygen atoms. Thus, $(PCA)_2 \subset AzaEx^2Cage \cdot 6PF_6$ exhibits axial chirality in the solid state, even though the two enantiomers co-crystallize in a racemic crystal lattice.

BH4EN, which is another π-electron-rich compound that bears two tetraethylene glycol chains grafted onto a 1,5-dioxynaphthalene (**DNP**) moiety, was also added into a CD_3CN solution of $AzaEx^2Cage \cdot 6PF_6$ in order to investigate their recognition behavior. Interestingly, instead of forming an inclusion complex in either a 1 : 1 or 1 : 2 manner, it seems that the external complex $BH4EN \cdot AzaEx^2Cage^{6+}$ is formed. This assumption was supported initially by the ^1H NMR spectrum (Fig. 1e). Upon addition of 11.4 equiv. of **BH4EN**, the resonance of the H_b proton in $BIPY^{2+}$ undergoes a significant upfield shift ($\Delta\delta \approx -0.229$ ppm), while those of H_c and H_d in the platforms are barely shifted. This observation indicates that, instead of undergoing π–π interactions with the cage platform, the **DNP** moiety prefers to interact with the $BIPY^{2+}$ pillars in the host, which therefore experiences a magnetically shielded environment. No NOESY cross-peaks between the phenylene units in the host platforms and **DNP** protons in the guest are observed in the NOESY spectrum (Fig. S27†) of the complex $BH4EN \cdot AzaEx^2Cage^{6+}$, indicating that the interactions between **DNP** and $BIPY^{2+}$ occur on the periphery of the cage molecule. The formation of external complex was unambiguously confirmed by single-crystal X-ray diffraction. In the solid state (Fig. 5), the face-to-face distance between **DNP** and $BIPY^{2+}$ is around 3.46 Å, confirming the occurrence of π-electron donor–acceptor interactions. The two glycol chains of the guest penetrate into the cavities of two adjacent cage molecules. The shortest contact between an oxygen atom in the glycol chain and one of the H_b protons in $BIPY^{2+}$ is around 2.24 Å, indicating the existence of [C–H···O] interactions. The combination of donor–acceptor and hydrogen-bonding interactions make the formation of the external complex more thermodynamically favorable than formation of the inclusion complex wherein the **DNP** guest undergoes π–π interactions with the triazine residue in the platforms. In water, the recognition mode for **BH4EN** and $AzaEx^2Cage^{6+}$ is similar, *i.e.*, adding **BH4EN** to a solution (1.0 mM) of $AzaEx^2Cage \cdot 6Cl$ in D_2O also results in an upfield shift of the resonances for the $BIPY^{2+}$ protons. However, an interesting difference is that strong NOESY cross-peaks between the **DNP** protons (H_y and/or H_z) and the phenylene protons (H_c and H_d) in the host platforms are observed (Fig. 6). These observations indicate that, in water, the complex $BH4EN \subset AzaEx^2Cage^{6+}$ may exist in the form of an inclusion complex instead of the external complex observed in CD_3CN. This observation could be explained by the fact, that in water where the hydrophobic effect becomes predominant, the formation of the inclusion complex is more thermodynamically favored than formation of the external complex. Our attempts to obtain single crystals of the complex $BH4EN \subset AzaEx^2Cage^{6+}$ from water proved unsuccessful, probably because of the relatively high aqueous solubilities of both the host $AzaEx^2Cage \cdot 6Cl$ and the guest **BH4EN**.

When both **PCA** and **BH4EN** are added to a CD_3CN solution of $AzaEx^2Cage \cdot 6PF_6$, inclusion and external complexation occur

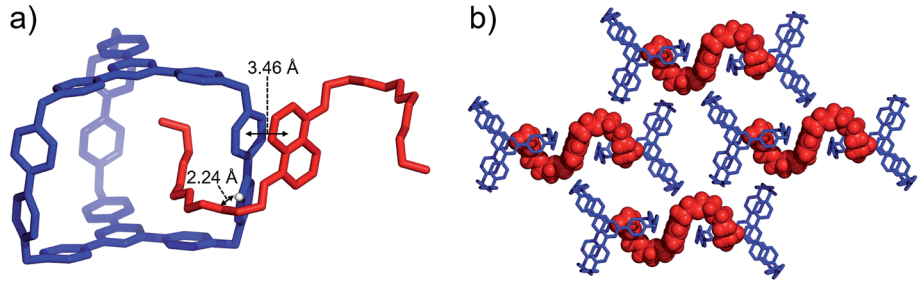

Fig. 5 (a) Side view of the crystal structure of the complex **BH4EN**·**AzaEx²Cage**·6PF_6 in the form of a stick diagram. (b) Top view of the complex **BH4EN**·**AzaEx²Cage**·6PF_6, showing that each **BH4EN** molecule interacts with two **BIPY**$^{2+}$ pillars in two adjacent cages. PF_6^- counterions are omitted for the sake of clarity.

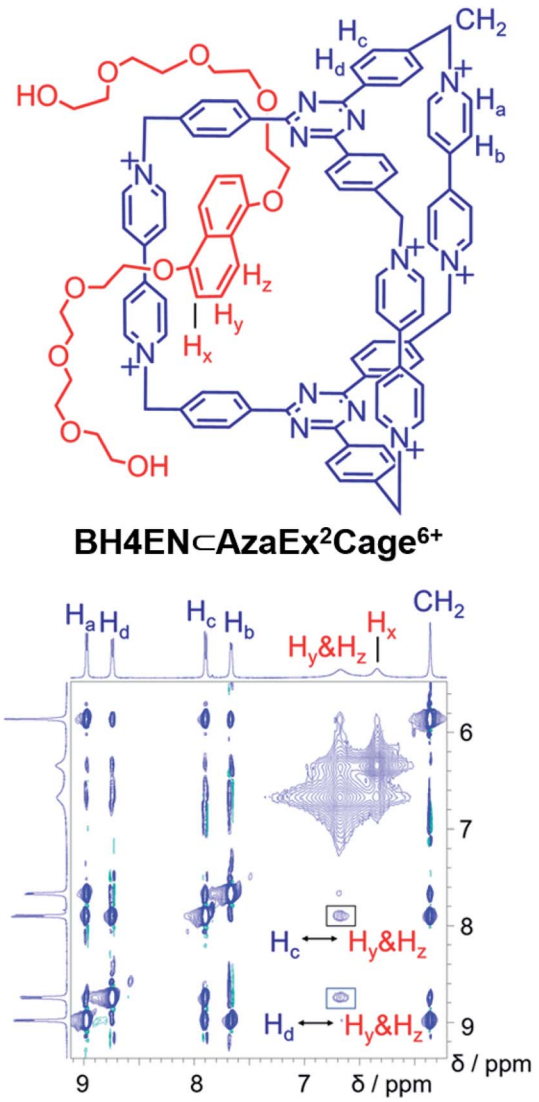

Fig. 6 ^{1}H–^{1}H NOESY spectrum of a 1 : 6 mixture of **AzaEx²Cage**·6Cl and **BH4EN** (500 MHz, D_2O, 298 K). Through-space proton couplings between the H_c and H_d protons in the phenylene groups of the cage and the H_y and/or H_z protons in the guests are labeled in the spectrum, demonstrating that **BH4EN**·**AzaEx²Cage**$^{6+}$ may exist in the form of an inclusion complex in water.

simultaneously, as inferred from the corresponding ^{1}H NMR spectroscopic analyses (Fig. S30–S33†), in which the proton resonances of both the platforms and pillars undergo shifts upon addition of **PCA** and **BH4EN**, respectively. Diffraction-grade single-crystals of **BH4EN**·(**PCA**)$_2$⊂**AzaEx²Cage**·6PF_6 were obtained by slow vapor diffusion of ^{i}Pr_2O into a three-component 10 : 4 : 1 mixture of **PCA**, **BH4EN** and **AzaEx²Cage**·6PF_6 in MeCN (2.0 mM) at 4 °C over a period of 3 days. In the solid state (Fig. 7), the cavity of a cage is occupied by two **PCA** guests, while a **BH4EN** guest resides on the external surface of a **BIPY**$^{2+}$ pillar in the host. The glycol chains of the **BH4EN** guest are excluded from the cage cavity by the two **PCA** guests. This observation implies that hydrogen bonding between the glycol chains and the **BIPY**$^{2+}$ units in the host might be attenuated to some extent in the solid state.

A ^{1}H NMR titration experiment was performed to evaluate the impact of **PCA** on the binding affinity of between **AzaEx²Cage**·6PF_6 and **BH4EN**. In the absence of **PCA**, the binding constant (K_a) for the complex **BH4EN**·**AzaEx²Cage**$^{6+}$ (Fig. S26 and S33†) is approximately around 36.7 ± 0.4 M^{-1} in CD_3CN, while upon adding 26.6 equiv. of **PCA**, the K_a value decreases to 4.9 ± 0.1 M^{-1}. The decrease of the binding constant in solution is consistent with the solid-state observation that encapsulation of **PCA** guests expels the glycol chains of **BH4EN** from the cage cavity and helps to decrease the strength of hydrogen bonding. Interestingly, in the presence of 7.8 equiv. of **BH4EN**, the binding constants between the cage and two **PCA** guests (Fig. S31†) seem to be barely changed as compared with those in the absence of **BH4EN**. We interprete this observation to mean that the impact of external binding on the environment inside the cage is of less importance.

Quantum mechanical calculations

In order to gain a better understanding of the recognition characteristics of **AzaEx²Cage**$^{6+}$ in terms of both inclusion and peripheral complexation, we have performed density functional theory (DFT) calculations to investigate the electronic properties **AzaEx²Cage**$^{6+}$. Geometry optimization of **AzaEx²Cage**$^{6+}$, **BH4EN**⊂**AzaEx²Cage**$^{6+}$, (pyrene)$_2$⊂**AzaEx²Cage**$^{6+}$, and (**PCA**)$_2$⊂**AzaEx²Cage**$^{6+}$ were performed at the M06-2X level of theory[22] with the 6-31G(d) basis set.[23] The single-point energies and solvent effects in MeCN were computed at the M06-2X level of theory with the 6-311++G(d,p) basis set for all the atoms, based on the

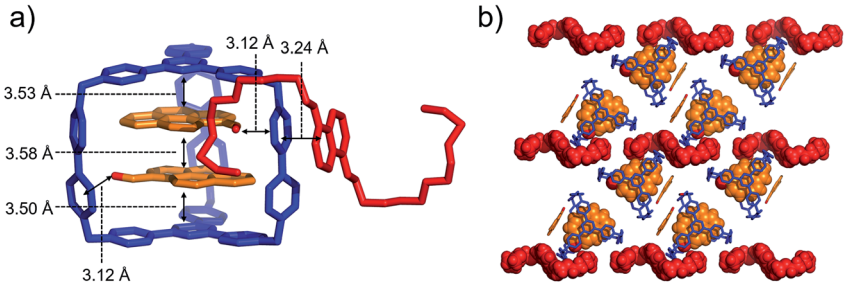

Fig. 7 (a) Side view of the crystal structure of the complex **BH4EN**·$(\mathbf{PCA})_2\subset$**AzaEx^{2}Cage**·6PF_6 in the form of a stick diagram. (b) Top view of the complex **BH4EN**·$(\mathbf{PCA})_2\subset$**AzaEx^{2}Cage**·6PF_6. PF_6^- counterions are omitted for the sake of clarity.

optimized gas-phase structures. Solvation energies were evaluated by a self-consistent reaction field (SCRF) using the SMD model.[24] Natural population analysis[25] of **AzaEx^{2}Cage**$^{6+}$ demonstrates that the bipyridinium, methylene and **TPT** units take +1.301, +0.327 and +0.074 (see the ESI†), respectively, implying that the **BIPY**$^{2+}$ pillars of the cage, including both pyridinium moieties and the methylene linkers, takes up most of the positive charge on the cage. Expressed another way, the **BIPY**$^{2+}$ pillars are more electron-deficient than the **TPT** platforms (Fig. 8a). On one hand, since the **DNP** unit in a **BH4EN** guest represents a π-electron-rich donor, it is not surprising that **DNP** prefers to interact with **BIPY**$^{2+}$, forming a **BH4EN·AzaEx^{2}Cage**$^{6+}$ complex (Fig. 8b) whose formation is also strengthened by hydrogen-bonding interactions. On the other hand, the guests pyrene and **PCA** have larger π-electron surfaces. As a consequence, they prefer to interact with the **TPT** platform driven by π–π stacking interactions as well as solvophobic effects. To visualize the cation–dipole interactions, we performed reduced density gradient (RDG) analysis[26] on the $(\mathbf{PCA})_2\subset$**AzaEx^{2}Cage**$^{6+}$. The analysis shows clearly the occurrence of noncovalent bonding interactions (Fig. S50†) between the formyl group on **PCA** and the viologen pillars in **AzaEx^{2}Cage**$^{6+}$.

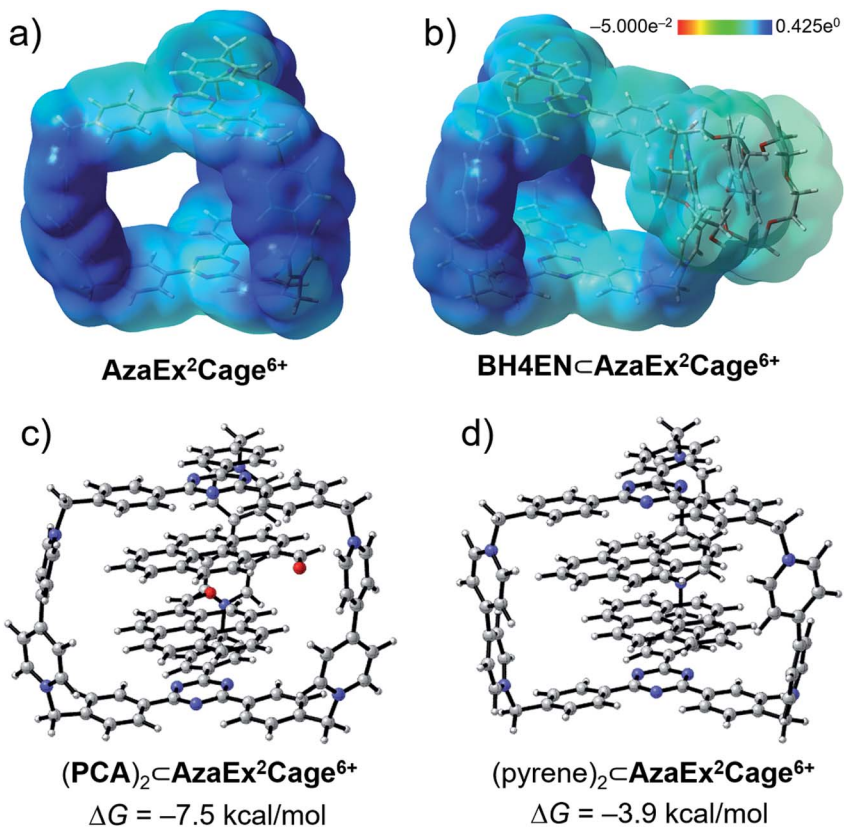

Fig. 8 Electrostatic potential maps for (a) **AzaEx^{2}Cage**$^{6+}$ and (b) **BH4EN**$\subset$**AzaEx^{2}Cage**$^{6+}$ obtained by using DFT calculations. Light-yellow and deep-blue colors in the maps represent negative and positive electrostatic potentials, respectively, demonstrating that the **BIPY**$^{2+}$ units represent better π-electron acceptors on account of their stronger π-electron deficiency. DFT-optimized structures of (c) $(\mathbf{PCA})_2\subset$**AzaEx^{2}Cage**$^{6+}$ and (d) $(\text{pyrene})_2\subset$**AzaEx^{2}Cage**$^{6+}$. The free energy changes (ΔG) for the formation of $(\mathbf{PCA})_2\subset$**AzaEx^{2}Cage**$^{6+}$ and $(\text{pyrene})_2\subset$**AzaEx^{2}Cage**$^{6+}$ complexes are calculated to be −7.5 and −3.9 kcal mol^{-1}, respectively.

DFT calculations were also performed to evaluate the free energy change (ΔG), which is defined as the free energy difference between the complex and the corresponding unbound guest and host (Fig. 8c and d), for the formation of (pyrene)$_2\subset$**AzaEx^{2}Cage**$^{6+}$ and (**PCA**)$_2\subset$**AzaEx^{2}Cage**$^{6+}$. The ΔG values for the formation of (pyrene)$_2\subset$**AzaEx^{2}Cage**$^{6+}$ and (**PCA**)$_2\subset$**AzaEx^{2}Cage**$^{6+}$ were calculated to be -3.9 and -7.5 kcal mol^{-1}, respectively. The more negative ΔG for (**PCA**)$_2\subset$**AzaEx^{2}Cage**$^{6+}$ indicates that its formation is more thermodynamically favored than that of (pyrene)$_2\subset$**AzaEx^{2}Cage**$^{6+}$. These results are consistent with the observations that the formation of the former complex is enhanced by dipole–cation or dipole–dipole interactions between the guest carbonyl oxygen atoms, which bear partially negative charges, and the dicationic **BIPY**$^{2+}$ units in the host.

Conclusion

In summary, we have introduced a hexacationic triangular prismatic cage that is composed of two **TPT** platforms connected by three **BIPY**$^{2+}$ pillar-shaped spacers. Both the platforms and the pillars play important roles in host–guest recognition. The cage can form 2 : 1 inclusion complexes with polycyclic aromatic hydrocarbons, including pyrene and **PCA**. The latter guest exhibits remarkably enhanced binding affinities within the cage cavity compared with those of the former, owing to dipole–cation and dipole–dipole interactions between the carbonyl groups and the laterally pillar-shaped spacers in the host. In addition, because the three **BIPY**$^{2+}$ pillars represent both an efficient π-electron acceptor and hydrogen bonding donor, one of them can interact with a **BH4EN** guest, which contains a π-electron-donating **DNP** unit and two hydrogen-bond-accepting glycol chains. External complexation occurs in organic solvents, while inclusion complexation can occur in water. When both **PCA** and **BH4EN** are present, both inclusion and peripheral complexation occur simultaneously, even though accommodation of the former guests seems to suppress the external binding of the latter.

These findings improve our fundamental understanding of the relationship between the electrostatic properties of the building blocks of supramolecular systems and their host–guest recognition properties. Specifically, laterally charged moieties within host molecules could supply effective intermolecular interaction to drive the inclusion and peripheral complexations. Furthermore, this work will inform the development of a design principle for more complex cage molecules that can bind guests in multiple modes and sites.

Conflicts of interest

There are no conflicts of interest to declare.

Acknowledgements

This work was supported by the Chinese "Thousand Youth Talents Plan", the National Natural Science Foundation of China (No. 21772173), the Natural Science Foundation of Zhejiang Province (No. LR18B020001). H. L. and T. J. also wish to express their appreciation for the financial support from Zhejiang University. Z. L. thanks Westlake University for the startup funds. J. F. S. expresses appreciation to King Abdulaziz City for Science and Technology (KACST) and Northwestern University (NU) for support of this work. We thank Prof. Xin Hong (Department of Chemistry, Zhejiang University) for his help with the computational resources used in this investigation.

References

1 A. Ikeda and S. Shinkai, *Chem. Rev.*, 1997, **97**, 1713–1734.
2 W. Maes and W. Dehaen, *Chem. Soc. Rev.*, 2008, **37**, 2393–2402.
3 P. Timmerman, W. Verboom and D. N. Reinhoudt, *Tetrahedron*, 1996, **52**, 2663–2704.
4 T. Ogoshi, S. Kanai, S. Fujinami, T. A. Yamagishi and Y. Nakamoto, *J. Am. Chem. Soc.*, 2008, **130**, 5022–5023.
5 P. A. Gale, P. Anzenbacher and J. L. Sessler, *Coord. Chem. Rev.*, 2001, **222**, 57–102.
6 (*a*) F. Diederich, *Angew. Chem., Int. Ed. Engl.*, 1988, **27**, 362–386; (*b*) M. Buhner, W. Geuder, W. K. Gries, S. Hunig, M. Koch and T. Poll, *Angew. Chem., Int. Ed. Engl.*, 1988, **27**, 1553–1556.
7 (*a*) B. Odell, M. V. Reddington, A. M. Z. Slawin, N. Spencer, J. F. Stoddart and D. J. Williams, *Angew. Chem., Int. Ed. Engl.*, 1988, **27**, 1547–1550; (*b*) P. R. Ashton, B. Odell, M. V. Reddington, A. M. Z. Slawin, J. F. Stoddart and D. J. Williams, *Angew. Chem., Int. Ed. Engl.*, 1988, **27**, 1550–1553.
8 (*a*) M. Asakawa, P. R. Ashton, S. Menzer, F. M. Raymo, J. F. Stoddart, A. J. P. White and D. J. Williams, *Chem.–Eur. J.*, 1996, **2**, 877–893; (*b*) P. R. Ashton, S. E. Boyd, A. Brindle, S. J. Langford, S. Menzer, L. Perez-Garcia, J. A. Preece, F. M. Raymo, N. Spencer, J. F. Stoddart, A. J. P. White and D. J. Williams, *New J. Chem.*, 1999, **23**, 587–602; (*c*) H. Y. Gong, B. M. Rambo, E. Karnas, V. M. Lynch and J. L. Sessler, *Nat. Chem.*, 2010, **2**, 406–409; (*d*) E. J. Dale, N. A. Vermeulen, M. Juríček, J. C. Barnes, R. M. Young, M. R. Wasielewski and J. F. Stoddart, *Acc. Chem. Res.*, 2016, **49**, 262–273; (*e*) E. J. Dale, D. P. Ferris, N. A. Vermeulen, J. J. Henkelis, I. Popovs, M. Juríček, J. C. Barnes, S. T. Schneebeli and J. F. Stoddart, *J. Am. Chem. Soc.*, 2016, **138**, 3667–3670; (*f*) X. Gong, R. M. Young, K. J. Hartlieb, C. Miller, Y. Wu, H. Xiao, P. Li, N. Hafezi, J. Zhou, L. Ma, T. Cheng, W. A. Goddard III, O. K. Farha, J. T. Hupp, M. R. Wasielewski and J. F. Stoddart, *J. Am. Chem. Soc.*, 2017, **139**, 4107–4116; (*g*) I. Roy, S. Bobbala, J. Zhou, M. T. Nguyen, S. K. M. Nalluri, Y. Wu, D. P. Ferris, E. A. Scott, M. R. Wasielewski and J. F. Stoddart, *J. Am. Chem. Soc.*, 2018, **140**, 7206–7212; (*h*) Y. Shi, K. Cai, H. Xiao, Z. C. Liu, J. W. Zhou, D. K. Shen, Y. Y. Qiu, Q. H. Guo, C. Stern, M. R. Wasielewski, F. Diederich, W. A. Goddard III and J. F. Stoddart, *J. Am. Chem. Soc.*, 2018, **140**, 13835–13842.
9 (*a*) C. A. Hunter and J. K. M. Sanders, *J. Am. Chem. Soc.*, 1990, **112**, 5525–5534; (*b*) L. M. Salonen, M. Ellermann and F. Diederich, *Angew. Chem., Int. Ed.*, 2011, **50**, 4808–4842.

10 (*a*) *Molecular Switches*, ed. B. L. Feringa, Wiley-VCH, Weinheim, 2001; (*b*) M. A. Olson, Y. Y. Botros and J. F. Stoddart, *Pure Appl. Chem.*, 2010, **82**, 1569–1574; (*c*) R. Klajn, J. F. Stoddart and B. A. Grzybowski, *Chem. Soc. Rev.*, 2010, **39**, 2203–2237; (*d*) Y. R. Hua and A. H. Flood, *J. Am. Chem. Soc.*, 2010, **132**, 12838–12840; (*e*) A. I. Share, K. Parimal and A. H. Flood, *J. Am. Chem. Soc.*, 2010, **132**, 1665–1675.

11 (*a*) B. L. Feringa, R. A. van Delden, N. Koumura and E. M. Geertsema, *Chem. Rev.*, 2000, **100**, 1789–1816; (*b*) R. Ballardini, V. Balzani, A. Credi, M. T. Gandolfi and M. Venturi, *Acc. Chem. Res.*, 2001, **34**, 445–455; (*c*) A. Harada, *Acc. Chem. Res.*, 2001, **34**, 456–464; (*d*) C. A. Schalley, K. Beizai and F. Vögtle, *Acc. Chem. Res.*, 2001, **34**, 465–476; (*e*) J. P. Collin, C. Dietrich-Buchecker, P. Gavina, M. C. Jimenez-Molero and J.-P. Sauvage, *Acc. Chem. Res.*, 2001, **34**, 477–487; (*f*) V. Balzani, A. Credi and M. Venturi, *Molecular Devices and Machines: A Journey into the Nanoworld*, 2nd edn, Wiley-VCH, Weinheim, 2006; (*g*) E. R. Kay, D. A. Leigh and F. Zerbetto, *Angew. Chem., Int. Ed.*, 2007, **46**, 72–191; (*h*) J. F. Stoddart, *Nat. Chem.*, 2009, **1**, 14–15; (*i*) M. M. Boyle, R. A. Smaldone, A. C. Whalley, M. W. Ambrogio, Y. Y. Botros and J. F. Stoddart, *Chem. Sci.*, 2011, **2**, 204–210; (*j*) C. Y. Cheng, P. R. McGonigal, S. T. Schneebeli, H. Li, N. A. Vermeulen, C. F. Ke and J. F. Stoddart, *Nat. Nanotechnol.*, 2015, **10**, 547–553.

12 (*a*) D. H. Qu, Q. C. Wang and H. Tian, *Angew. Chem., Int. Ed.*, 2005, **44**, 5296–5299; (*b*) H. Zheng, W. Zhou, J. Lv, X. Yin, Y. Li, H. Liu and Y. Li, *Chem.–Eur. J.*, 2009, **15**, 13253–13262; (*c*) Q. Jiang, H. Y. Zhang, M. Han, Z. J. Ding and Y. Liu, *Org. Lett.*, 2010, **12**, 1728–1731; (*d*) C. Romuald, E. Busseron and F. Coutrot, *J. Org. Chem.*, 2010, **75**, 6516–6531.

13 (*a*) A. Livoreil, C. O. Dietrich-Buchecker and J.-P. Sauvage, *J. Am. Chem. Soc.*, 1994, **116**, 9399–9400; (*b*) M. Asakawa, P. R. Ashton, V. Balzani, A. Credi, C. Hamers, G. Mattersteig, M. Montalti, A. N. Shipway, N. Spencer, J. F. Stoddart, M. S. Tolley, M. Venturi, A. J. P. White and D. J. Williams, *Angew. Chem., Int. Ed.*, 1998, **37**, 333–337; (*c*) D. Cao, M. Amelia, L. M. Klivansky, G. Koshkakaryan, S. I. Khan, M. Semeraro, S. Silvi, M. Venturi, A. Credi and Y. Liu, *J. Am. Chem. Soc.*, 2010, **132**, 1110–1122; (*d*) J. C. Barnes, A. C. Fahrenbach, D. Cao, S. M. Dyar, M. Frasconi, M. A. Giesener, D. Benítez, E. Tkatchouk, O. Chernyashevskyy, W. H. Shin, H. Li, S. Sampath, C. L. Stern, A. A. Sarjeant, K. J. Hartlieb, Z. C. Liu, R. Carmieli, Y. Y. Botros, J. W. Choi, A. M. Z. Slawin, J. B. Ketterson, M. R. Wasielewski, W. A. Goddard III and J. F. Stoddart, *Science*, 2013, **339**, 429–433.

14 E. J. Dale, N. A. Vermeulen, A. A. Thomas, J. C. Barnes, M. Juríček, A. K. Blackburn, N. L. Strutt, A. A. Sarjeant, C. L. Stern, S. E. Denmark and J. F. Stoddart, *J. Am. Chem. Soc.*, 2014, **136**, 10669–10682.

15 (*a*) M. Juríček, N. L. Strutt, J. C. Barnes, A. M. Butterfield, E. J. Dale, K. K. Baldridge, F. Stoddart and J. S. Siegel, *Nat. Chem.*, 2014, **6**, 222–228; (*b*) B. M. Schmidt, T. Osuga, T. Sawada, M. Hoshino and M. Fujita, *Angew. Chem., Int. Ed.*, 2016, **55**, 1561–1564.

16 (*a*) P. R. Ashton, C. L. Brown, E. J. T. Chrystal, T. T. Goodnow, A. E. Kaifer, K. P. Parry, D. Philp, A. M. Z. Slawin, N. Spencer, J. F. Stoddart and D. J. Williams, *J. Chem. Soc., Chem. Commun.*, 1991, 634–639; (*b*) M. V. Reddington, A. M. Z. Slawin, N. Spencer, J. F. Stoddart, C. Vicent and D. J. Williams, *J. Chem. Soc., Chem. Commun.*, 1991, 630–634.

17 (*a*) B. E. Tiedemann and K. N. Raymond, *Angew. Chem., Int. Ed.*, 2005, **45**, 83–86; (*b*) C. Sgarlata, J. S. Mugridge, M. D. Pluth, B. E. Tiedemann, V. Zito, G. Arena and K. N. Raymond, *J. Am. Chem. Soc.*, 2010, **132**, 1005–1009; (*c*) T. Sawada and M. Fujita, *J. Am. Chem. Soc.*, 2010, **132**, 7194–7201; (*d*) W. J. Ramsay and J. R. Nitschke, *J. Am. Chem. Soc.*, 2014, **136**, 7038–7043; (*e*) F. J. Rizzuto, W. Y. Wu, T. K. Ronson and J. R. Nitschke, *Angew. Chem., Int. Ed.*, 2016, **55**, 7958–7962; (*f*) D. Preston, J. E. Lewis and J. D. Crowley, *J. Am. Chem. Soc.*, 2017, **139**, 2379–2386; (*g*) X. Bai, C. Jia, Y. Zhao, D. Yang, S. C. Wang, A. Li, Y. T. Chan, Y. Y. Wang, X. J. Yang and B. Wu, *Angew. Chem., Int. Ed.*, 2018, **57**, 1851–1855.

18 J. Samanta and R. Natarajan, *Org. Lett.*, 2016, **18**, 3394–3397.

19 (*a*) M. Yoshizawa, J. Nakagawa, K. Kumazawa, M. Nagao, M. Kawano, T. Ozeki and M. Fujita, *Angew. Chem., Int. Ed.*, 2005, **44**, 1810–1813; (*b*) M. M. Zhang, M. L. Saha, M. Wang, Z. X. Zhou, B. Song, C. J. Lu, X. Z. Yan, X. P. Li, F. H. Huang, S. C. Yin and P. J. Stang, *J. Am. Chem. Soc.*, 2017, **139**, 5067–5074.

20 A. Trabolsi, N. Khashab, A. C. Fahrenbach, D. C. Friedman, M. T. Colvin, K. K. Coti, D. Benítez, E. Tkatchouk, J. C. Olsen, M. E. Belowich, R. Carmielli, H. A. Khatib, W. A. Goddard III, M. R. Wasielewski and J. F. Stoddart, *Nat. Chem.*, 2010, **2**, 42–49.

21 N. Hafezi, J. M. Holcroft, K. J. Hartlieb, E. J. Dale, N. A. Vermeulen, C. L. Stern, A. A. Sarjeant and J. F. Stoddart, *Angew. Chem., Int. Ed.*, 2015, **54**, 456–461.

22 (*a*) Y. Zhao and D. G. Truhlar, *Acc. Chem. Res.*, 2008, **41**, 157–167; (*b*) Y. Zhao and D. G. Truhlar, *Theor. Chem. Acc.*, 2008, **120**, 215–241.

23 W. J. Hehre, L. Radom, P. v. R. Schleyer and J. A. Pople, *Ab Initio Molecular Orbital Theory*, Wiley, New York, 1986.

24 A. V. Marenich, C. J. Cramer and D. G. Truhlar, *J. Phys. Chem. B*, 2009, **113**, 6378–6396.

25 A. E. Reed, R. B. Weinstock and F. Weinhold, *J. Chem. Phys.*, 1985, **83**, 735–746.

26 E. R. Johnson, S. Keinan, P. Mori-Sanchez, J. Contreras-Garcia, A. J. Cohen and W. T. Yang, *J. Am. Chem. Soc.*, 2010, **132**, 6498–6506.